Density Matrix Topological Insulators

A. Rivas, O. Viyuela and M. A. Martin-Delgado
Departamento de Fisica Teorica I, Universidad Complutense, 28040 Madrid, Spain.

Thermal noise can destroy topological insulators (TI). However we demonstrate how TIs can be made stable in dissipative systems. To that aim, we introduce the notion of a band Liouvillian as the dissipative counterpart of a band Hamiltonian, and show a method to evaluate the topological order of its steady state. This is based on a generalization of the Chern number valid for general mixed states (referred as density matrix Chern value), which witnesses topological order in a system coupled to external noise. Additionally, we study its relation with the electrical conductivity at finite temperature, which is not topologically invariant. Nonetheless, the density matrix Chern value represents the part of the conductivity which is topological due to the presence of quantum mixed edge states at finite temperature. To make our formalism concrete, we apply these concepts to the two-dimensional Haldane model in the presence of thermal dissipation, but our results hold for arbitrary dimensions and density matrices.

PACS numbers: 73.43.Cd, 03.65.Yz, 03.65.Vf 73.20.At

Introduction.— In a recent work [1], we have shown that certain one-dimensional topological insulators (TI) lose the topological protection of their edge states when they are coupled to bosonic thermal baths. This is so even when the bath interaction preserves the symmetry that protects the existence of edge states. As a consequence, these edge states decay in time into bulk states of a normal insulator. Thus, a very fundamental question arises: is it possible to have stable topological insulating states in the presence of a thermal bath? The purpose of this letter is to explore this possibility by extending the concept of TI [2–5] to dissipative systems. Since for dissipative systems quantum states are generally mixed and characterized by a density matrix operator ρ, we shall refer to these as *density matrix TI.*

For usual TIs, the TKNN invariant [6] provides a characterization of fermionic topological order. This is done in such a way that the transverse conductivity is written in terms of a topological invariant, the Chern number, which may be related to an adiabatic change of the Hamiltonian in momentum space [7]. However the extension of this invariant to density matrices is not straightforward. Actually, the problem of generalizing geometric concepts as distances or geometric phases to generally mixed states is highly non-trivial [8–12]. We address this problem and construct an observable that detects the topological order of a TI even if it is not in a pure, but in a general quantum mixed state. Moreover, when this general quantum state is of the form of a Gibbs state, we study the relation between this topological observable and the conductivity, and show that it reduces to the usual notion of TI in the limit of low temperature. However, we stress that the notion of a density matrix TI is far more general, as we shall see.

This letter is completed with a supplementary information document (SM) where we include most of the technical details.

Chern Connections for Density Matrices.— The physical problem is defined as follows. Let $H_{\rm s}$ be the system Hamiltonian representing a certain TI. This could be constructed in an arbitrary spatial dimension, but we shall restrict in what follows to the class of time reversal broken (TRB) insulators in two spatial dimensions. Furthermore, the TI will be subjected to the action of dissipative effects due to a thermal bath represented by a Hamiltonian $H_{\rm b}$. This bath could be general enough so as to comprise fermionic or bosonic degrees of freedom and we assume it is initially in a thermal or Gibbs state at a certain temperature T. The system-bath interaction is described by the Hamiltonian $H_{\rm s-b}$.

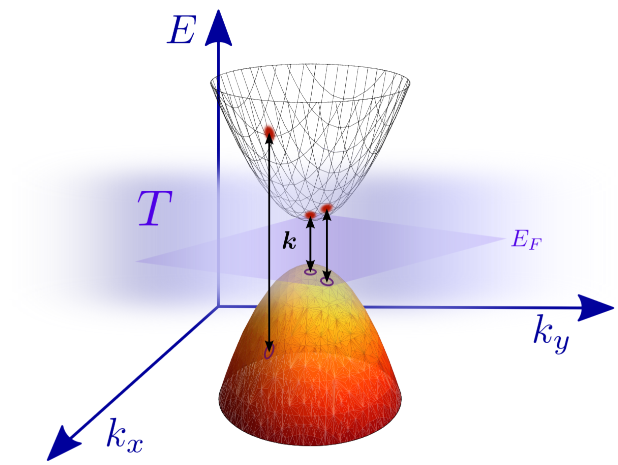

Figure 1: Pictorial image of the action of a band Liouvillian $\mathcal{L}=\sum_{\boldsymbol{k}}\mathcal{L}_{\boldsymbol{k}}$. The vertical lines denote the only possible processes involving the (initially empty) conduction band and (initially filled) valence bands, i.e. the ones where the momentum $\boldsymbol{k}$ is preserved. The violet fog represents some bath at a certain temperature T which mediate such a processes (see Eq. (5)) and the plane indicate the Fermi energy E_F.

We consider that the state $\rho_{\rm s}$ of the TI undergoes a time evolution satisfying some Lindblad dynamical equation [13–16] (unless otherwise stated, natural units

$\hbar = k_B = 1$ are taken throughout the paper):

$$\frac{\mathrm{d}\rho_{\mathrm{s}}}{\mathrm{d}t} = \mathcal{L}(\rho_{\mathrm{s}}) = -\mathrm{i}[H_{\mathrm{s}}, \rho_{\mathrm{s}}] + \mathcal{D}(\rho_{\mathrm{s}}), \tag{1}$$

where $\mathcal{L}$ is the so-called *Liouvillian* operator, which is composed by a first term representing the Hamiltonian evolution in the absence of system-bath interaction and a second term accounting for the effect of the bath dissipation. Concretely, we shall assume that $\mathcal{L}$ is of the Davies type, obtained under the assumption of weak system-bath coupling [17].

We are interested in searching for sufficient conditions that the Liouvillian dynamics (1) must satisfy in order to preserve the TI phase. In the absence of dissipation, we know that a key ingredient is that the TI Hamiltonian H_{s} is a band Hamiltonian that satisfies the Bloch theorem and can be decomposed as $H_{\mathrm{s}} = \sum_{\boldsymbol{k}\in\mathrm{B.Z.}} H_{\mathrm{s}}(\boldsymbol{k})$ where $\boldsymbol{k}$ denotes a crystalline momentum. Thus, it is natural to restrict our attention to Liouvillian evolutions satisfying a similar condition, $\mathcal{L} = \sum_{\boldsymbol{k}\in\mathrm{B.Z.}} \mathcal{L}_{\boldsymbol{k}}$; we shall refer to these as *band Liouvillians*. Basically, a Liouvillian of this kind describes processes in such a way that the momenta of the fermions are not changed (up to a vector $\mathbf{G}$ of the reciprocal lattice), a pictorial image is sketched in Fig. 1. As a consequence, they present invariance under space translations, which imposes the following constraints (see section 1 of SM) on its associated steady states $\rho_{\mathrm{ss}}, \mathcal{L}(\rho_{\mathrm{ss}}) = 0$:

$$\rho_{\mathrm{ss}} = \bigotimes_{\boldsymbol{k}} \rho_{\mathrm{ss}}^{\boldsymbol{k}}, \quad \rho_{\mathrm{ss}}^{\boldsymbol{k}} := \lambda_0|0\rangle\langle 0| + \sum_{\alpha,\beta} \lambda_{\alpha\beta}^{\boldsymbol{k}} |1_{\alpha,\boldsymbol{k}}\rangle\langle 1_{\beta,\boldsymbol{k}}|. \tag{2}$$

Here, $|1_{\alpha,\boldsymbol{k}}\rangle \equiv |u_{\alpha,\boldsymbol{k}}\rangle$ denotes a particle of type α in the Bloch state with momentum $\boldsymbol{k}$ associated with the system Hamiltonian H_{s}, where α, β account for other internal indexes, such as band indexes (like valence and conduction band) or spin indexes. The coefficients $\lambda_{\alpha\beta}^{\boldsymbol{k}}$ depend on the particular steady state as a result of the dissipative dynamics (1). For instance, if the steady state turns out to be a thermal state density matrix, then they will be given by Gibbs weights (8).

In order to construct a topological invariant for the generally mixed state $\rho_{\mathrm{ss}}^{\boldsymbol{k}}$, we cannot use the usual Berry connection as in the formulation of the Chern number, because it is defined just for pure states. Regarding density matrices, there is not a unique natural extension of the Berry connection and the Berry phase [8–12]. However, the band Liouvillian structure allows us for the construction of a Berry-type connection A_i^{ρ} for the density matrix steady states, in such a way that the integral of its curvature form, F_{ij}^{ρ}, gives a topological invariant which we refer to as *density matrix Chern value*. Thus, one of the main results of this work is the construction of this invariant $\mathrm{n}_{\mathrm{Ch}}^{\rho}$, which characterizes the topological structure of insulators in the presence of dissipation and can be written as

$$\begin{aligned}\mathrm{n}_{\mathrm{Ch}}^{\rho} =& \frac{1}{2\pi}\int_{\mathrm{T}^2} F_{12}^{\rho} d^2k = \frac{1}{2\pi}\sum_{\alpha}\int_{\mathrm{T}^2} p_{\alpha}^{\boldsymbol{k}} F_{12}^{\alpha} d^2k \\ &+ \frac{1}{2\pi}\sum_{\alpha}\int_{\mathrm{T}^2}\left[\left(\partial_1 p_{\alpha}^{\boldsymbol{k}}\right) A_2^{\alpha}(\boldsymbol{k}) - \left(\partial_2 p_{\alpha}^{\boldsymbol{k}}\right) A_1^{\alpha}(\boldsymbol{k})\right] d^2k.\end{aligned} \tag{3}$$

Here, $p_{\alpha}^{\boldsymbol{k}}$ are the eigenvalues of $\rho_{\mathrm{ss}}^{\boldsymbol{k}}$ in (2) and $A_i^{\alpha}(\boldsymbol{k})$ are the Berry connections of each band. We refer to the SM (section 2) for the detailed derivation and notation. A non-varnishing $\mathrm{n}_{\mathrm{Ch}}^{\rho}$ witnesses a topological non-trivial order present in $\rho_{\mathrm{ss}}^{\boldsymbol{k}}$. When the steady state is a pure Bloch state $\rho_{\mathrm{ss}}^{\boldsymbol{k}} = |u_{\alpha,\mathbf{k}}\rangle\langle u_{\alpha,\mathbf{k}}|$, we recover the standard TKNN topological invariant (Chern number).

The density matrix Chern value $\mathrm{n}_{\mathrm{Ch}}^{\rho}$, Eq. (3), has two different terms. The first one is a weighted integration of curvatures for different bands. This term has no topological meaning on its own and it does not distinguish between phases with or without topological order. The second term represents a correction to the value given by the first one that provides the topological character to $\mathrm{n}_{\mathrm{Ch}}^{\rho}$. In addition, both terms have a physical meaning which will be explained later on.

The name *Chern value* responds the fact that despite its topological origin, it may not be an integer for a general mixed state. The reason is very fundamental; the space of density matrices ρ is a convex space, which means that a convex combination of density matrices ρ_1 and ρ_2, $\rho = p_1\rho_1 + p_2\rho_2$ is also a mixed state. Due to the abelian character of the curvature form F_{ij}^{ρ} (see sec-

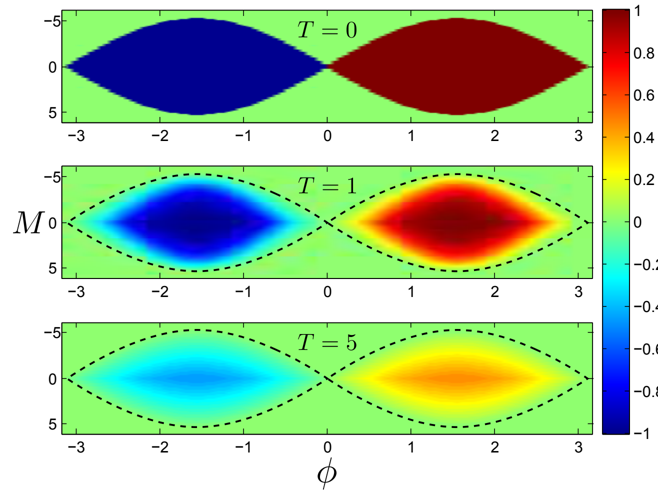

Figure 2: Colormap depicting the Chern value in the Haldane model with dissipation, for different values of ϕ, M and bath temperature T (in units of $t_2 = 1$). As T increases the Chern value decreases (in absolute value), and for $T = 0$ we recover the phase diagram obtained by Haldane [18]. The dashed black lines enclosures the region displaying topological order at $T = 0$, so that all nonvanishing Chern values are inside of this region for any T. Approximately $T = 1$ and $T = 5$ correspond to less than 10% and 50% of the gap respectively.

tion 2 of SM), $\mathrm{n}_{\mathrm{Ch}}^{\rho} = p_1 \mathrm{n}_{\mathrm{Ch}}^{\rho_1} + p_2 \mathrm{n}_{\mathrm{Ch}}^{\rho_2}$. Therefore, since the weights $p_1, p_2 \in \mathbb{R}$ with $p_1 + p_2 = 1$, then $\mathrm{n}_{\mathrm{Ch}}^{\rho} \in \mathbb{R}$ as well. Nevertheless, this will be not an obstacle to use the Chern value to detect topological properties in insulator states. We will see this explicitly in the case of the Haldane model in 2D which is a prototype of TRB topological insulator [18].

Band Liouvillian for the Haldane Model.— We can apply our previous formalism to the Haldane model of 2D TI. This is a graphene-like model based on a honeycomb lattice with nearest-neighbors and next-nearest-neighbors couplings. For periodic boundary conditions the Haldane Hamiltonian in the reciprocal space is given by

$$H_{\mathrm{s}} = \sum_{\boldsymbol{k}\in\mathrm{B.Z.}} (a_{\boldsymbol{k}}^\dagger, b_{\boldsymbol{k}}^\dagger) H(\boldsymbol{k}) \begin{pmatrix} a_{\boldsymbol{k}} \\ b_{\boldsymbol{k}} \end{pmatrix} = \sum_{\boldsymbol{k}\in\mathrm{B.Z.}} E_1^{\boldsymbol{k}} c_{\boldsymbol{k}}^\dagger c_{\boldsymbol{k}} + E_2^{\boldsymbol{k}} d_{\boldsymbol{k}}^\dagger d_{\boldsymbol{k}}. \tag{4}$$

Here, $a_{\boldsymbol{k}}$ and $b_{\boldsymbol{k}}$ correspond to the two species of fermions associated with the triangular sublattices of a honeycomb lattice, and $c_{\boldsymbol{k}}$ and $d_{\boldsymbol{k}}$ are the femionic modes which diagonalize the Hamiltonian with eigenvalues $E_1^{\boldsymbol{k}}$ and $E_2^{\boldsymbol{k}}$ respectively. For more details we refer to section 3 of the SM.

We shall assume a local fermionic bath model, with quadratic coupling of the form

$$H_{\mathrm{s-b}} := \sum_{i,\boldsymbol{r}} g^i (a_{\boldsymbol{r}}^\dagger \otimes A_{\boldsymbol{r}}^i + a_{\boldsymbol{r}} \otimes A_{\boldsymbol{r}}^{i\dagger} + b_{\boldsymbol{r}}^\dagger \otimes B_{\boldsymbol{r}}^i + b_{\boldsymbol{r}} \otimes B_{\boldsymbol{r}}^{i\dagger}), \tag{5}$$

where $\boldsymbol{r}$ denotes the point in the sublattices and $A_{\boldsymbol{r}}^i$ and $B_{\boldsymbol{r}}^i$ the bath fermion operators coupled with the two species $a_{\boldsymbol{r}}$ and $b_{\boldsymbol{r}}$ respectively.

The detailed derivation of the Liouvillian equation (master equation) in the weak coupling limit for this systems is explained in section 4 of SM; the final result turns out to be

$$\begin{aligned}
\frac{d\rho_{\mathrm{s}}(t)}{dt} &= \sum_{\boldsymbol{k}} \mathcal{L}_{\boldsymbol{k}}[\rho_{\mathrm{s}}(t)] = \sum_{\boldsymbol{k}} \bigg(-\mathrm{i}[H_{\boldsymbol{k}}, \rho_{\mathrm{s}}(t)] \\
&+ \gamma(E_1^{\boldsymbol{k}}) \bar{n}_F(E_1^{\boldsymbol{k}}) \Big(c_{\boldsymbol{k}}^\dagger \rho_{\mathrm{s}}(t) c_{\boldsymbol{k}} - \frac{1}{2}\{c_{\boldsymbol{k}} c_{\boldsymbol{k}}^\dagger, \rho_{\mathrm{s}}(t)\} \Big) + \\
&+ \gamma(E_1^{\boldsymbol{k}}) [1 - \bar{n}_F(E_1^{\boldsymbol{k}})] \Big(c_{\boldsymbol{k}} \rho_{\mathrm{s}}(t) c_{\boldsymbol{k}}^\dagger - \frac{1}{2}\{c_{\boldsymbol{k}}^\dagger c_{\boldsymbol{k}}, \rho_{\mathrm{s}}(t)\} \Big) \\
&+ \gamma(E_2^{\boldsymbol{k}}) \bar{n}_F(E_2^{\boldsymbol{k}}) \Big(d_{\boldsymbol{k}}^\dagger \rho_{\mathrm{s}}(t) d_{\boldsymbol{k}} - \frac{1}{2}\{d_{\boldsymbol{k}} d_{\boldsymbol{k}}^\dagger, \rho_{\mathrm{s}}(t)\} \Big) + \\
&+ \gamma(E_2^{\boldsymbol{k}}) [1 - \bar{n}_F(E_2^{\boldsymbol{k}})] \Big(d_{\boldsymbol{k}} \rho_{\mathrm{s}}(t) d_{\boldsymbol{k}}^\dagger - \frac{1}{2}\{d_{\boldsymbol{k}}^\dagger d_{\boldsymbol{k}}, \rho_{\mathrm{s}}(t)\} \Big) \bigg).
\end{aligned} \tag{6}$$

Here,

$$\bar{n}_F(E) := \frac{1}{\mathrm{e}^{\beta E} + 1}, \quad \gamma(\omega) := 2\pi J(\omega), \tag{7}$$

where $J(\omega)$ is the bath spectral density.

It is important to emphasize that this Liouvillian (6) fulfills the conditions of a band Liouvillian $\mathcal{L} = \sum_{\boldsymbol{k}\in\mathrm{B.Z.}} \mathcal{L}_{\boldsymbol{k}}$. Moreover, it is quadratic in fermionic operators and its unique steady state is the Gibbs state ($\beta = 1/T$)

$$\rho_\beta = \frac{\mathrm{e}^{-\beta H_{\mathrm{s}}}}{Z} = \bigotimes_{\boldsymbol{k}} \rho_{\mathrm{ss}}^{\boldsymbol{k}} = \bigotimes_{\boldsymbol{k}} \left(\frac{\mathrm{e}^{-\beta E_1^{\boldsymbol{k}} c_{\boldsymbol{k}}^\dagger c_{\boldsymbol{k}}}}{1 + \mathrm{e}^{-\beta E_1^{\boldsymbol{k}}}} \right) \left(\frac{\mathrm{e}^{-\beta E_2^{\boldsymbol{k}} d_{\boldsymbol{k}}^\dagger d_{\boldsymbol{k}}}}{1 + \mathrm{e}^{-\beta E_2^{\boldsymbol{k}}}} \right), \tag{8}$$

that has the form of (2) corresponding to a band Liouvillian. Note that in the limit $T \to 0$, ρ_β approaches the Fermi sea where the lower band ($c_{\boldsymbol{k}}$) is fully occupied and the upper band ($d_{\boldsymbol{k}}$) is completely empty (see section 5 of SM for more details).

Chern Value of the Steady State.— We have obtained that the steady state of the Liuvillian (6) is a product of states $\rho_{\mathrm{ss}}^{\boldsymbol{k}}$ with well-defined momentum. Thus, the (parallel) transport along $\boldsymbol{k}$-*space* of each of these states is well defined, and hence, the state characterization by a density matrix Chern value (3) is possible.

For the sake of computation, note that $\rho_{\mathrm{ss}}^{\boldsymbol{k}}$ is diagonal in the occupation basis $\rho_{\mathrm{ss}}^{\boldsymbol{k}} = \sum_{n,m\in\{0,1\}} p_{nm}^{\boldsymbol{k}} |m,n\rangle_{\boldsymbol{k}} \langle m,n|$, where

$$\begin{aligned}
|00\rangle_{\boldsymbol{k}} &= |0\rangle|0\rangle, & |10\rangle_{\boldsymbol{k}} &= |u_{c,\boldsymbol{k}}\rangle|0\rangle, \\
|01\rangle_{\boldsymbol{k}} &= |0\rangle|u_{d,\boldsymbol{k}}\rangle, & |11\rangle_{\boldsymbol{k}} &= |u_{c,\boldsymbol{k}}\rangle|u_{d,\boldsymbol{k}}\rangle.
\end{aligned}$$

The vacuum $|0\rangle$ has no particles and does not depend on $\boldsymbol{k}$. If we define the geometric connections for the lower (c) and upper (d) bands:

$$A_i^\alpha(\boldsymbol{k}) := \mathrm{i}\langle u_{\alpha,\boldsymbol{k}} | \partial_i u_{\alpha,\boldsymbol{k}} \rangle, \quad \alpha = c, d, \tag{9}$$

then it is possible to express the connection $A_i^\rho(\boldsymbol{k})$ in terms of the previous ones (see section 5 of SM):

$$A_i^\rho(\boldsymbol{k}) = \bar{n}_F(E_1^{\boldsymbol{k}}) A_i^c(\boldsymbol{k}) + \bar{n}_F(E_2^{\boldsymbol{k}}) A_i^d(\boldsymbol{k}). \tag{10}$$

Note that in the $T \to 0$ limit, we recover the standard Berry connection $A_i^\rho(\boldsymbol{k}) \to A_i^c(\boldsymbol{k})$, as the steady state (8) approaches the Fermi sea with the fully occupied lower band.

The Chern value can be now computed by integrating the curvature form of $A_i^\rho(\boldsymbol{k})$ (or by using the simplified expression (3)). The colormap in Fig. 2 represents the Chern value for different values of M and ϕ and different bath temperatures. Note its nice properties: it is zero for any choice of M and ϕ for all temperatures if it is zero at $T = 0$. This manifests that the topological order cannot be created by increasing temperature. Moreover, as T increases, the absolute value of the Chern value decreases, and in the limit of $T \to \infty$ we obtain $\mathrm{n}_{\mathrm{Ch}}^{\rho} \to 0$ for all M and ϕ. This is in agreement with the common intuition that at infinite temperature any kind of order should be spoiled.

Dissipative Edge States and Master Equation.— A physical signature of a TI phase is the existence of gapless (metallic) edge states. Thus, once we have mathematically characterized the phase diagram of the Haldane model under dissipation by means of the density matrix

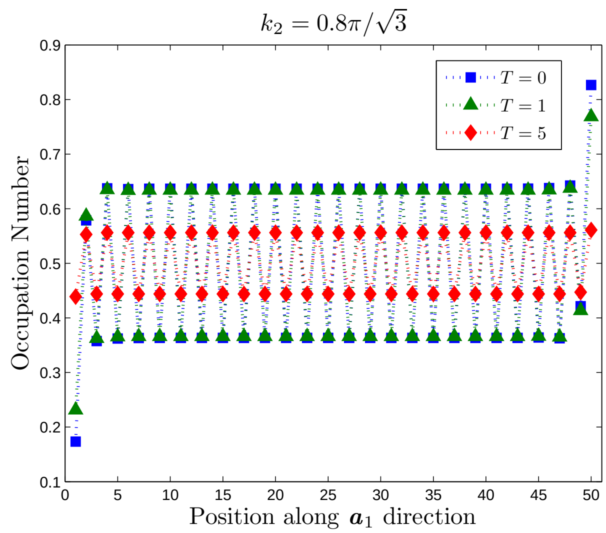

Figure 3: Occupation along the direction $\boldsymbol{a}_1$ for all particles with momentum $k_2 = \frac{4}{5}\frac{\pi}{|\boldsymbol{a}_2|}$, $M = 0$ and $\phi = \pi/2$), for different values of T (in units of $t_2 = 1$). Note the presence of edge states at finite temperature, Eq. (16), in the positions 1 and 50 along the direction $\boldsymbol{a}_1$. Note the presence of edge states at finite temperature, . However, as the temperature T increases significantly the population of the edge modes becomes similar to the population of the bulk modes.

Chern value, we wonder about the fate of the chiral edge states of the Haldane model at finite temperature.

To that aim, we consider the Haldane model placed on a cylindrical geometry, where we take periodic boundary conditions just along one spatial dimension, say $\boldsymbol{a}_2$. In such a case the momentum k_2 along the $\boldsymbol{a}_2$ direction is a good quantum number and the Haldane Hamiltonian can be diagonalized obtaining (see section 3 of SM for more details)

$$H_{\mathrm{s}} = \sum_{k_2 \in \mathrm{B.Z.}} H(k_2) = \sum_{k_2 \in \mathrm{B.Z.}} E_m^{k_2} f_{m,k_2}^\dagger f_{m,k_2}, \tag{11}$$

Here, the diagonal modes f_{m,k_2} mix both species of fermions a_{m,k_2} and b_{m,k_2}.

By imposing this geometry also in the interaction Hamiltonian (5), we derive the following dynamical equation for the system (see section 4 of SM)

$$\begin{aligned}\frac{d\rho_{\mathrm{s}}(t)}{dt} &= \sum_{k_2 \in \mathrm{B.Z.}} \mathcal{L}_{k_2}[\rho_{\mathrm{s}}(t)] = \sum_{k_2 \in \mathrm{B.Z.}} \Bigg(-\mathrm{i}[H(k_2), \rho_{\mathrm{s}}(t)] \\ &+ \sum_m \Big(\gamma\big(E_m^{k_2}\big) \bar{n}_F\big(E_m^{k_2}\big) \mathcal{D}_{f^\dagger_{(m,k_2)}}[\rho_{\mathrm{s}}(t)] \\ &+ \gamma\big(E_m^{k_2}\big)\big[1 - \bar{n}_F\big(E_m^{k_2}\big)\big] \mathcal{D}_{f_{(m,k_2)}}[\rho_{\mathrm{s}}(t)]\Big)\Bigg),\end{aligned} \tag{12}$$

where

$$\mathcal{D}_K[\rho_{\mathrm{s}}(t)] := K\rho_{\mathrm{s}}(t)K^\dagger - \frac{1}{2}\{K^\dagger K, \rho_{\mathrm{s}}(t)\}. \tag{13}$$

Again, the Gibbs state at the same temperature as the bath is the unique steady state of Eq. (12),

$$\rho_\beta = \frac{\mathrm{e}^{-\beta \sum_{k_2} H(k_2)}}{Z} = \bigotimes_{k_2} \frac{\mathrm{e}^{-\beta H(k_2)}}{Z_{k_2}}, \tag{14}$$

with $Z_{k_2} = \mathrm{Tr}\left[\mathrm{e}^{-\beta H(k_2)}\right]$. Therefore, as long as the values of M, t_2 and ϕ are such that the system exhibits topological order (see Fig. 2), two of the modes which diagonalize each $H(k_2)$, say $f_{(L,k_2)}$ and $f_{(R,k_2)}$, correspond to edge states and the Gibbs state is a tensor product in k_2 of states of the form

$$\rho_\beta(k_2) = \frac{\mathrm{e}^{-\beta H(k_2)}}{Z_{k_2}} = \rho_\beta^{\mathrm{L}}(k_2) \otimes \rho_\beta^{\mathrm{bulk}}(k_2) \otimes \rho_\beta^{\mathrm{R}}(k_2), \tag{15}$$

where

$$\rho_\beta^{\mathrm{L,R}}(k_2) := \frac{\mathrm{e}^{-\beta E_{L,R}(k_2) f^\dagger_{(L,R,k_2)} f_{(L,R,k_2)}}}{1 + \mathrm{e}^{-\beta E_{L,R}(k_2)}}, \tag{16}$$

are Gibbs states of the edge modes. However as temperature increases (see again Fig. 2) the edge modes in the steady state of the Liouvillian (12) become delocalized. Then the components $\rho^{\mathrm{L,R}}(k_2)$ approach to a maximally mixed state with vacuum $|0\rangle$. In such a situation, there is not a way to distinguish the edge from the bulk modes, because for all k_2 the occupation along the direction $\boldsymbol{a}_1$ becomes the same and equal to $1/2$. We illustrate this behavior in Fig. 3.

It is worth stressing that in order to study the dissipative effects on the cylindrical Haldane system we must determine how the boundary conditions of the system affect the dissipator operator. To that aim we need to specify how the dissipator is generated (constructed). In our case this is the result of the weak interaction of the system with local baths. However there are also possible scenarios where the dissipator is the effective result of other external interactions (see for example [19–23]). Since the process of "opening" or "closing" a system has a physical meaning, we stress that we need to know how the dissipator is physically generated to obtain its "open" and/or "closed" counterpart. Note that a dissipator with periodic boundary conditions, may split in different and nonequivalent dissipators once the system is opened along some direction if it is generated in different ways.

Quantum Hall Conductivity and Chern Value at Finite Temperature.— We can obtain further physical meaning and implications for the density matrix Chern value (3) by studying the (quantum Hall) transverse conductivity σ_{xy} and its relation to the thermal edge states obtained for the Haldane model. Using the Kubo formula [24] in linear response theory, it is possible to derive an expression for the transverse Hall conductivity at finite temperature [25]:

$$\sigma_{xy}^{\rho} = \frac{e^2}{2\pi h} \sum_\alpha \int_{\mathrm{T}^2} \bar{n}_F(E_\alpha^{\boldsymbol{k}}) F_{xy}^\alpha(\boldsymbol{k}) d^2\boldsymbol{k}. \tag{17}$$

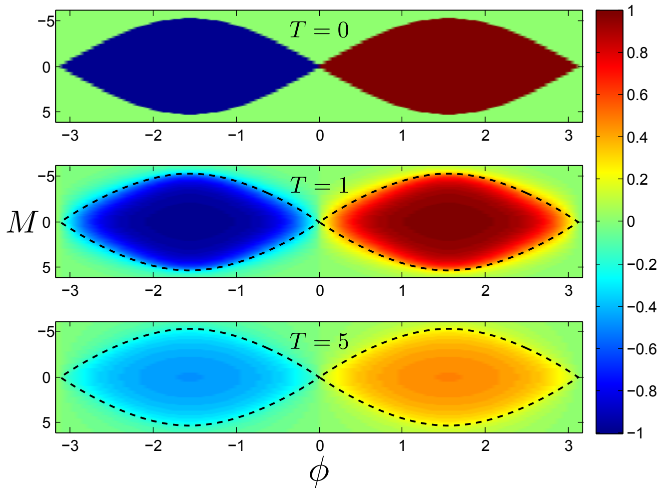

Figure 4: Colormap depicting the conductivity Eq. (17) for different values of ϕ, M and the bath temperature T (in units of $t_2 = 1$). As T increases the conductivity decreases (in absolute value), and for $T = 0$ we recover the Chern number result, Fig. 2. The dashed black lines enclosures the region displaying topological order at $T = 0$. Thus, contrarily to the Chern value, the conductivity is not topologically invariant for finite T, as it does not vanish for every point outside this region for any T.

Note that this expression [26] is different from the one obtained for the Chern value (3). Indeed, the conductivity is not topological at finite temperature, as shown in Fig. 4 where non-zero Hall conductivity appears in regions outside the topological regime, in contrast with Fig. 2. Nonetheless, both quantities can be related by means of the following equation:

$$\sigma^{\rho}_{xy} = \frac{e^2}{h}\mathrm{n}^{\rho}_{\mathrm{Ch}} + \frac{e^2}{2\pi h}\sum_{\alpha}\int_{\mathrm{T}^2}\Big[(\partial_y p^{\boldsymbol{k}}_{\alpha})A^{\alpha}_{x}(\boldsymbol{k}) - (\partial_x p^{\boldsymbol{k}}_{\alpha})A^{\alpha}_{y}(\boldsymbol{k})\Big]d^2\boldsymbol{k}. \tag{18}$$

The second term on the right hand side of (18) is the same one that appears for the transverse conductivity of a normal insulator with an applied magnetic field (or a pseudo-magnetic field as for the Haldane model) at $T \neq 0$. It corresponds to the conduction by thermal activation of excited electrons in the bulk. For instance, for parameters $t_1 = 4, t_2 = 1, \phi = \frac{\pi}{2}$ and $M = 6$ in the Haldane model, this term is the only non-zero contribution to the conductivity, as the system is outside the topological regime, and so $\mathrm{n}^{\rho}_{\mathrm{Ch}} = 0$.

Notwithstanding, the first term on the right hand side of (18), which is nothing but the Chern value previously defined, represents a contribution due to the topological nature of our system and the presence of conducting edge states. For parameters $t_1 = 4, t_2 = 1, \phi = \frac{\pi}{2}$ and $M = 0$ in the Haldane model, the system is within the topological regime and this new term shows up. Note that at $T = 0$ we recover the well known TKNN expression for the conductivity:

$$\sigma^{\rho}_{xy} \xrightarrow[T\longrightarrow 0]{} \frac{e^2}{h}\,\nu_{\mathrm{Ch}}, \tag{19}$$

where ν_{Ch} denotes the standard Chern number.

Conclusions.— We have studied topological insulating phases in the presence of dissipation. After introducing the notion of band Liouvillian, we address the characterization of the topological order of its steady states by resorting to the density matrix Chern value, a topological invariant that is an extension of the Chern number for pure states. The Haldane model of a 2D TI in contact with a thermal bath offers a nice testbed to study these phenomena. More concretely, we compute phase diagrams at finite temperature based on the Chern value, and corroborate that topological order decreases as the bath temperature increases. Thus, from a topologically disordered state it is not possible induce a topologically ordered phase just by warming the system. However a topologically ordered state may remain ordered at finite temperature T except at the limit $T \to \infty$. This has to be compared with the previous study [1] where the topological order turned out to be lost for a dissipative system in the presence of noise not generated by a band Liouvillian. Our results may also have direct application in recent studies regarding dissipation on Majorana fermions in topological superconductors [20, 27].

Complementarily, we study the properties of the Haldane model coupled to a thermal bath under cylindrical boundary conditions. We find that the the steady state splits in three different, generally mixed substates Eq. (15), two of them are associated with creation or annihilation of fermionic gapless edge modes, and the other one accounts for the same process just in the bulk modes. In the limit $T \to 0$ we recover the properties of the usual Haldane model.

Finally, we examine the relation between the density matrix Chern value and the conductivity at finite temperature. We show that the latter is not topologically invariant, in contrast to the Chern value. This fact is due to the presence of an extra term which accounts for the conductivity generated by thermal activation of electrons in the bulk, which has not a particular topological meaning and is present in normal insulators. In this regard, provided that the gap between conduction and valence bands is large enough, the Chern value may be approximately estimated by measuring the conductivity, as the thermal activation would be very small. However, recent results [28], suggest that a direct measurement of the density matrix Chern value could be possible in optical lattice realizations.

Acknowledgements –. We thank Alexandre Dauphin for fruitful discussions. This work has been supported by the Spanish MINECO grant FIS2012-33152, CAM research consortium QUITEMAD S2009-ESP-1594, European Commission PICC: FP7 2007-2013, Grant No. 249958, UCM-BS grant GICC-910758.

[1] O. Viyuela, A. Rivas, and M. A. Martin-Delgado, Phys. Rev. B **86**, 155140 (2012).
[2] M. Z. Hasan and C. L. Kane, Rev. Mod. Phys. **82**, 3045 (2010).
[3] X.-L. Qi and S.-C. Zhang, Rev. Mod. Phys. **83**, 1057 (2011).
[4] X.-L. Qi and S.-C. Zhang, Phys. Today **63**, 33 (2010).
[5] J. E. Moore, Nature **464**, 194 (2010).
[6] D. J. Thouless, M. Kohmoto, P. Nightingale and M. den Nijs. Phys. Rev. Lett. **49**, 405 (1982); M. Kohmoto Ann. Phys. NY **160**, 343 (1985); Phys. Rev. B **39**, 11943 (1989).
[7] Y. Hatsugai, J. Phys.: Condens. Matter **9**, 2507 (1997).
[8] A. Uhlmann, Rep. Math. Phys. **24**, 229 (1986); **36**, 461 (1995).
[9] E. Sjöqvist, A. K. Pati, A. Ekert, J. S. Anandan, M. Ericsson, D. K. L. Oi and V. Vedral, Phys. Rev. Lett. **85**, 2845 (2000).
[10] S. Filipp and E. Sjöqvist, Phys. Rev. Lett. **90**, 050403 (2003).
[11] M. Ericsson, A. K. Pati, E. Sjöqvist, J. Brännlund and D. K. L. Oi, Phys. Rev. Lett. **91**, 090405 (2003).
[12] K. Singh, D. M. Tong, K. Basu, J. L. Chen and J. F. Du, Phys. Rev. A **67**, 032106 (2003).
[13] R. Alicki and K. Lendi, *Quantum Dynamical Semigroups and Applications* (Springer, Berlin, 1987).
[14] C.W. Gardiner and P. Zoller, *Quantum Noise* (Springer, Berlin, 1991).
[15] H.-P. Breuer and F. Petruccione, *The Theory of Open Quantum Systems* (Oxford University Press, 2002).
[16] A. Rivas and S.F. Huelga, *Open Quantum Systems. An Introduction* (Springer, Heidelberg, 2011).
[17] E. B. Davies, Comm. Math. Phys. **39**, 91 (1974); Math. Ann. **219**,147 (1976).
[18] F.D.M. Haldane, Phys. Rev. Lett. **61**, 2015 (1988).
[19] F. Verstraete, M. M. Wolf and J. I. Cirac, Nature Phys. **5**, 633 (2009).
[20] S. Diehl, E. Rico, M. A. Baranov and P. Zoller, Nature Phys. 7, 971977 (2011).
[21] M. Müller, S. Diehl, G. Pupillo and P. Zoller, Adv. Atom. Mol. Opt. Phy. **61**, 1 (2012).
[22] B. Horstmann, J. I. Cirac and G. Giedke, Phys. Rev. A **87**, 012108 (2013).
[23] J. Eisert and T. Prosen, arXiv:1012.5013.
[24] R. Kubo, J. Phys. Soc. Jap. **12**, 570 (1957).
[25] D. Xiao, M-C. Chang, Q. Niu, Rev. Mod. Phys. **82**, 1959-2007 (2010).
[26] Note that in this formula we have restored the units e (electron charge) and h (Planck constant) as it is customary in this context.
[27] L. Mazza, M. Rizzi, M. D. Lukin and J. I. Cirac, arXiv:1212.4778.
[28] M. Atala, M. Aidelsburger, J. T. Barreiro, D. Abanin, T. Kitagawa, E. Demler and I. Bloch, arXiv:1212.0572; D. A. Abanin, T. Kitagawa, I. Bloch and E. Demler, arXiv:1212.0562.

SUPLEMENTARY MATERIAL

1. Band Liouvillian Dynamics

There are some natural requirements to be imposed on a Liouvillian $\mathcal{L}$ in order to generalize the theory of TIs as developed for band Hamiltonians $H_{\rm s} = \sum_{\boldsymbol{k}\in \text{B.Z.}} H_{\rm s}(\boldsymbol{k})$ where $\boldsymbol{k}$ denotes a crystalline momentum. In analogy to these, we introduce the class of band Liouvillians, which by definition are those that can be decomposed as $\mathcal{L} = \sum_{\boldsymbol{k}\in \text{B.Z.}} \mathcal{L}_{\boldsymbol{k}}$, where each $\mathcal{L}_{\boldsymbol{k}}$ only involves fermionic operators with the crystalline momentum $\boldsymbol{k}$. A band Liouvillian presents translational invariance, as every $\mathcal{L}_{\boldsymbol{k}}$ is translationally invariant:

$$T(\boldsymbol{a})\mathcal{L}_{\boldsymbol{k}}(\rho)T^\dagger(\boldsymbol{a}) = \mathcal{L}_{\boldsymbol{k}}\left[T(\boldsymbol{a})\rho T^\dagger(\boldsymbol{a})\right], \tag{S1}$$

where $T(\boldsymbol{r}) = \mathrm{e}^{-\mathrm{i}\boldsymbol{a}\cdot\hat{\boldsymbol{k}}}$ is the operator that translates a point with coordinate $\boldsymbol{r}$ to the point $\boldsymbol{r}+\boldsymbol{a}$ on the lattice.

An analogous to the Bloch theorem for this kind of Liovillians characterizes its steady states.

Theorem 1 *Consider a band Liouvillian $\mathcal{L} = \sum_{\boldsymbol{k}\in \text{B.Z.}} \mathcal{L}_{\boldsymbol{k}}$. If each $\mathcal{L}_{\boldsymbol{k}}$ has a unique stationary state, it has the form*

$$\rho_{\rm ss} = \lambda_0 |0\rangle\langle 0| + \sum_{\boldsymbol{k},\alpha,\beta} \lambda^{\boldsymbol{k}}_{\alpha\beta} |1_{\alpha,\boldsymbol{k}}\rangle\langle 1_{\beta,\boldsymbol{k}}|. \tag{S2}$$

Here, α and β denote additional quantum numbers (band indexes, spin indexes, lattice indexes, etc.), and $|1_{\alpha,\boldsymbol{k}}\rangle \equiv |u_{\alpha,\boldsymbol{k}}\rangle$ denotes a particle in the Bloch state with momentum $\boldsymbol{k}$ and additional quantum number α, $T(\boldsymbol{r})|u_{\alpha,\boldsymbol{k}}\rangle = \mathrm{e}^{-\mathrm{i}\boldsymbol{r}\cdot\boldsymbol{k}}|u_{\alpha,\boldsymbol{k}}\rangle$.

Proof: Consider $\rho_{\rm ss}$ to be the steady state of some $\mathcal{L}_{\boldsymbol{k}}$:

$$\mathcal{L}_{\boldsymbol{k}}(\rho_{\rm ss}) = 0. \tag{S3}$$

By applying the translation operator on both sides and using (S1), we obtain

$$\mathcal{L}_{\boldsymbol{k}}\left[T(\boldsymbol{a})\rho_{\rm ss} T^\dagger(\boldsymbol{a})\right] = 0. \tag{S4}$$

Thus, $\rho'_{\rm ss} := T(\boldsymbol{a})\rho_{\rm ss}T^\dagger(\boldsymbol{a})$ is also a steady state of the system. Since by assumption $\rho_{\rm ss}$ is unique, $\rho'_{\rm ss} = \rho_{\rm ss}$, so that $[T(\boldsymbol{a}), \rho_{\rm ss}] = 0$ and $T(\boldsymbol{a})$ and $\rho_{\rm ss}$ share the same eigenvectors. □

It is worth noticing that as a difference with the case of pure states, the translational symmetry of a Liovillian does not necessarily implies steady states with well-defined crystalline momentum $\boldsymbol{k}$. They can be a convex mixture of states with different well-defined momenta (S2). However, since the subspace with well-defined momentum $\boldsymbol{k}$ is invariant under the action of $\mathcal{L}_{\boldsymbol{k}}$, if the initial state has a well-defined momentum $\boldsymbol{k}$ (for instance a particle with well-defined momentum in one of the bands of the Hamiltonian), then the steady state under $\mathcal{L}_{\boldsymbol{k}}$ will have well-defined momentum as well,

$$\rho^{\boldsymbol{k}}_{\rm ss} = \lambda_0 |0\rangle\langle 0| + \sum_{\alpha,\beta} \lambda^{\boldsymbol{k}}_{\alpha\beta} |1_{\alpha,\boldsymbol{k}}\rangle\langle 1_{\beta,\boldsymbol{k}}|. \tag{S5}$$

Thus, the steady state of the total Liouvillian $\mathcal{L} = \sum_{\boldsymbol{k}\in \text{B.Z.}} \mathcal{L}_{\boldsymbol{k}}$ has the form of

$$\rho_{\rm ss} = \bigotimes_{\boldsymbol{k}} \rho^{\boldsymbol{k}}_{\rm ss}. \tag{S6}$$

2. Purified Topological Invariants for Band Liouvillians

Purification is a method that allows us to extend quantities defined for pure states to general mixed states. For a density matrix ρ acting in a Hilbert space $\mathcal{H}$, a purification $|\Phi^\rho\rangle$ is a pure state in an extended Hilbert space $|\Phi^\rho\rangle \in \mathcal{H}_A \otimes \mathcal{H}$ such that

$$\rho = \mathrm{Tr}_A\left(|\Phi^\rho\rangle\langle\Phi^\rho|\right). \tag{S7}$$

In other words, mixed states can always be seen as pure states of a larger system such that we only have access to partial information of it.

Given some ρ there are infinitely many states $|\Phi^\rho\rangle$ which fulfill (S7). Without loss of (mathematical) generality, it can be assumed that the ancillary space $\mathcal{H}_A$ (which physically may represent the thermal bath) has the same dimension d as $\mathcal{H}$ for the system, then any purification $|\Phi^\rho\rangle$ can be written as

$$|\Phi^\rho\rangle = (U_A \otimes \tilde{\rho})|\Omega\rangle, \tag{S8}$$

where U_A is a unitary operator, $\tilde{\rho}\tilde{\rho}^\dagger = \rho$ and

$$|\Omega\rangle := \sum_{\alpha=1}^{d} |v_\alpha\rangle \otimes |v_\alpha\rangle, \tag{S9}$$

is a maximally entangled state, with $\{|v_j\rangle\}$ an orthonormal basis of $\mathcal{H}$. From the Schmidt decomposition of $|\Phi^\rho\rangle$ it follows that (S8) is the most general form for a purification of ρ [1].

By using the spectral decomposition of $\rho = \sum_\alpha p_\alpha |\psi_\alpha\rangle\langle\psi_\alpha|$, we may write $\tilde{\rho}$ as

$$\tilde{\rho} = \sum_\alpha \sqrt{p_\alpha}|\psi_\alpha\rangle\langle\varphi_\alpha|, \tag{S10}$$

where $\{|\varphi_\alpha\rangle\}$ is also an orthonormal basis which is considered to be arbitrary. Therefore, given some ρ there is a freedom for the choice of U_A and the basis $\{|\varphi_\alpha\rangle\}$ for its purification $|\Phi^\rho\rangle$.

The next theorem is the main result of this section.

Theorem 2 *Consider the steady state of a band Liouvillian, Eq. (S6), we define a Berry-like connection for $\rho^{\boldsymbol{k}}_{\rm ss}$ through one of its purifications $|\Phi^\rho_{\boldsymbol{k}}\rangle$ as*

$$A^\rho_i(\boldsymbol{k}) := \mathrm{i}\langle\Phi^\rho_{\boldsymbol{k}}|\partial_i\Phi^\rho_{\boldsymbol{k}}\rangle, \quad \textit{for} \quad \rho^{\boldsymbol{k}}_{\rm ss} = \mathrm{Tr}_A\left(|\Phi^\rho_{\boldsymbol{k}}\rangle\langle\Phi^\rho_{\boldsymbol{k}}|\right). \tag{S11}$$

Here, the notation is $\partial_i := \partial_{k_i}$. Under the assumption that U_A and $\{|\varphi_i\rangle\}$ are independent of momentum $\boldsymbol{k}$ of

the steady state, the connection (S11) *is unique and does not depend on the purification. Explicitly, it takes the following form in terms of the spectral decomposition of* $\rho_{\rm ss}^{\boldsymbol{k}} = \sum_\alpha p_\alpha^{\boldsymbol{k}} |\psi_{\alpha,\boldsymbol{k}}\rangle\langle\psi_{\alpha,\boldsymbol{k}}|$*:*

$$A_i^\rho(\boldsymbol{k}) = \mathrm{i}\sum_\alpha p_\alpha^{\boldsymbol{k}} \langle\psi_{\alpha,\boldsymbol{k}}|\partial_i\psi_{\alpha,\boldsymbol{k}}\rangle. \tag{S12}$$

Proof: Indeed, the general form (S8) for a purification of $\rho_{\rm ss}^{\boldsymbol{k}}$ reads

$$|\Phi_{\boldsymbol{k}}^\rho\rangle = \sum_\alpha \sqrt{p_\alpha^{\boldsymbol{k}}}\,(U_A \otimes |\psi_{\alpha,\boldsymbol{k}}\rangle\langle\varphi_\alpha|)\,|\Omega\rangle, \tag{S13}$$

where we have used (S10). Taking the derivative $\partial_i := \partial_{k_i}$ in (S13) and computing the overlap

$$\langle\Phi_{\boldsymbol{k}}^\rho|\partial_i\Phi_{\boldsymbol{k}}^\rho\rangle = \sum_{\alpha,\beta}\sqrt{p_\beta^{\boldsymbol{k}}}\langle\Omega| \left[\left(\partial_i\sqrt{p_\alpha^{\boldsymbol{k}}}\right)(\mathbb{1}\otimes|\varphi_\beta\rangle\langle\psi_{\beta,\boldsymbol{k}}|\psi_{\alpha,\boldsymbol{k}}\rangle\langle\varphi_\alpha|) + \sqrt{p_\alpha^{\boldsymbol{k}}}\,(\mathbb{1}\otimes|\varphi_\beta\rangle\langle\psi_{\beta,\boldsymbol{k}}|\partial_i\psi_{\alpha,\boldsymbol{k}}\rangle\langle\varphi_\alpha|)\right]|\Omega\rangle. \tag{S14}$$

Since $\langle\Omega|(\mathbb{1}\otimes A)|\Omega\rangle = \mathrm{Tr}(A)$, we obtain

$$A_i^\rho(\boldsymbol{k}) = \mathrm{i}\sum_\alpha \sqrt{p_\alpha^{\boldsymbol{k}}}\left(\partial_i\sqrt{p_\alpha^{\boldsymbol{k}}}\right) + p_\alpha^{\boldsymbol{k}}\langle\psi_{\alpha,\boldsymbol{k}}|\partial_i\psi_{\alpha,\boldsymbol{k}}\rangle, \tag{S15}$$

which is independent of U_A and $\{|\varphi_i\rangle\}$. Moreover, note that in the pure state case $\rho_{\rm ss}^{\boldsymbol{k}} = |\psi_{\boldsymbol{k}}\rangle\langle\psi_{\boldsymbol{k}}|$ we recover the Berry connection $A_i^\rho(\boldsymbol{k}) = A_i(\boldsymbol{k}) = \mathrm{i}\langle\psi_{\boldsymbol{k}}|\partial_i\psi_{\boldsymbol{k}}\rangle$ [2]. In addition, the first term on the right hand side of (S15) vanishes by taking into account that $\sum_\alpha p_\alpha^{\boldsymbol{k}} = 1$. Hence, (S15) can written simply as (S12). □

Once this *purified connection* (S12) is defined, we may obtain the (abelian) curvature form through

$$F_{ij}^\rho(\boldsymbol{k}) := \partial_i A_j(\boldsymbol{k}) - \partial_j A_i(\boldsymbol{k}), \tag{S16}$$

and construct a density matrix topological invariant $\mathrm{n}_{\rm Ch}^\rho$ associated with the steady state $\rho_{\rm ss}^{\boldsymbol{k}}$ via the first Chern class [3] of this connection,

$$\mathrm{n}_{\rm Ch}^\rho := \frac{1}{2\pi}\mathrm{Tr}\left[\int_{\mathrm{T}^2} F_{ij}^\rho(\boldsymbol{k})dk_i\wedge dk_j\right]. \tag{S17}$$

It is convenient to compute the different contributions that appear in the explicit expression of (S16) after using (S12). We obtain

$$F_{ij}^\rho(\boldsymbol{k}) = \sum_\alpha\left[p_\alpha^{\boldsymbol{k}}F_{ij}^\alpha + \left(\partial_i p_\alpha^{\boldsymbol{k}}\right)A_j^\alpha(\boldsymbol{k}) - \left(\partial_j p_\alpha^{\boldsymbol{k}}\right)A_i^\alpha(\boldsymbol{k})\right]. \tag{S18}$$

Note that from this equation is not manifestly clear the $U(1)$ gauge invariance of the curvature, but this can be proven by performing a gauge transformation and making use of the property $\sum_\alpha p_\alpha^{\boldsymbol{k}} = 1$. However, the gauge invariance is more straightforwardly shown by noticing the clear gauge character of the connection (S11).

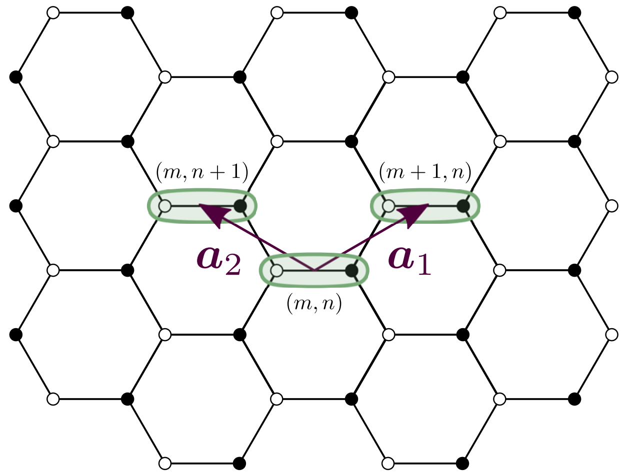

Figure S1: System of coordinates $\{\boldsymbol{a}_1, \boldsymbol{a}_2\}$ taken to write the Haldane Hamiltonian in real space (S19) . The solid white and black circles denote fermions a and b respectively, and the green enclosures highlight the two-site unit cell.

3. Haldane Model Geometries

In order to write explicitly the Haldane Hamiltonian [4] in real space we will consider the system of coordinates $\{\boldsymbol{a}_1, \boldsymbol{a}_2\}$ represented in Fig. S1, with $\boldsymbol{a}_1 = \frac{1}{2}(3, \sqrt{3})$ and $\boldsymbol{a}_2 = \frac{1}{2}(-3, \sqrt{3})$ for lattice spacing $a = 1$. We write $a_{(m,n)}$ ($b_{(m,n)}$) for the fermionic operator of kind a (b) in the position $\boldsymbol{r}_{(m,n)} = m\boldsymbol{a}_1 + n\boldsymbol{a}_2$. Then, the Haldane Hamiltonian in real space reads

$$\begin{aligned} H_{\rm s} := \sum_{m,n}\Bigg(& \tfrac{M}{2}[a^\dagger_{(m,n)}a_{(m,n)} - b^\dagger_{(m,n)}b_{(m,n)}] \\ & + t_1\left[a^\dagger_{(m,n)}b_{(m,n)} + a^\dagger_{(m+1,n)}b_{(m,n)} + a^\dagger_{(m,n)}b_{(m,n+1)}\right] \\ & + t_2\Big[\mathrm{e}^{\mathrm{i}\phi}a^\dagger_{(m,n)}a_{(m+1,n+1)} + \mathrm{e}^{-\mathrm{i}\phi}a^\dagger_{(m,n)}a_{(m+1,n)} \\ & + \mathrm{e}^{-\mathrm{i}\phi}a^\dagger_{(m,n)}a_{(m,n+1)} + \mathrm{e}^{-\mathrm{i}\phi}b^\dagger_{(m,n)}b_{(m+1,n+1)} \\ & + \mathrm{e}^{\mathrm{i}\phi}b^\dagger_{(m,n)}b_{(m+1,n)} + \mathrm{e}^{\mathrm{i}\phi}b^\dagger_{(m,n)}b_{(m,n+1)}\Big] + \mathrm{h.c.}\Bigg). \end{aligned} \tag{S19}$$

a. Toroidal Geometry

By taking periodic boundary conditions in both spatial directions, we may write the Hamiltonian (S19) in the reciprocal space using the Fourier-transformed operators

$$a_{(n,m)} = \frac{1}{\sqrt{N}}\sum_{\boldsymbol{k}\in\mathrm{B.Z.}} \mathrm{e}^{\mathrm{i}\boldsymbol{k}\cdot\boldsymbol{r}_{(m,n)}}a_{\boldsymbol{k}}, \tag{S20}$$

$$b_{(n,m)} = \frac{1}{\sqrt{N}}\sum_{\boldsymbol{k}\in\mathrm{B.Z.}} \mathrm{e}^{\mathrm{i}\boldsymbol{k}\cdot\boldsymbol{r}_{(m,n)}}b_{\boldsymbol{k}}, \tag{S21}$$

where B.Z. stands for Brillouin zone which is a hexagon with vertices in the $\boldsymbol{k} = (k_1, k_2)$ points

$$\left(0, \tfrac{4\pi}{3\sqrt{3}}\right), \left(\tfrac{2\pi}{3}, \tfrac{2\pi}{3\sqrt{3}}\right), \left(\tfrac{2\pi}{3}, -\tfrac{2\pi}{3\sqrt{3}}\right), \tag{S22}$$

$$\left(0, -\tfrac{4\pi}{3\sqrt{3}}\right), \left(-\tfrac{2\pi}{3}, -\tfrac{2\pi}{3\sqrt{3}}\right), \left(-\tfrac{2\pi}{3}, \tfrac{2\pi}{3\sqrt{3}}\right), \tag{S23}$$

and N is the total number of two-site unit cells. Thus the Haldane Hamiltonian is rewritten as

$$H_{\rm s} = \sum_{\boldsymbol{k}} (a_{\boldsymbol{k}}^\dagger \ , \ b_{\boldsymbol{k}}^\dagger) H(\boldsymbol{k}) \begin{pmatrix} a_{\boldsymbol{k}} \\ b_{\boldsymbol{k}} \end{pmatrix}. \tag{S24}$$

Here,

$$\begin{aligned} H_{11}(\boldsymbol{k}) &= M + 2t_2 \sum_i \cos[\phi + (\boldsymbol{k}\cdot\boldsymbol{b}_i)], \\ H_{12}(\boldsymbol{k}) &= H(\boldsymbol{k})_{21}^* = t_1 \sum_i \mathrm{e}^{-\mathrm{i}\boldsymbol{k}\cdot\boldsymbol{a}_i}, \\ H_{22}(\boldsymbol{k}) &= -M + 2t_2 \sum_i \cos[\phi - (\boldsymbol{k}\cdot\boldsymbol{b}_i)] \end{aligned} \tag{S25}$$

with

$$\begin{aligned} \boldsymbol{b}_1 &= -\left(3, \sqrt{3}\right)/2, \\ \boldsymbol{b}_2 &= \left(3, -\sqrt{3}\right)/2, \\ \boldsymbol{b}_3 &= \left(0, \sqrt{3}\right). \end{aligned} \tag{S26}$$

By diagonalizing the matrix $H(\boldsymbol{k})$ we obtain

$$H_{\rm s} = \sum_{\boldsymbol{k}} E_1^{\boldsymbol{k}} c_{\boldsymbol{k}}^\dagger c_{\boldsymbol{k}} + E_2^{\boldsymbol{k}} d_{\boldsymbol{k}}^\dagger d_{\boldsymbol{k}}, \tag{S27}$$

where the eigenvalues are given by

$$E_{1,2}^{\boldsymbol{k}} = 2t_2(\cos\phi)\ \delta_1(\boldsymbol{k}) \mp \sqrt{\Delta(\boldsymbol{k})} \tag{S28}$$

with

$$\begin{aligned} \Delta(\boldsymbol{k}) :=\ & M^2 + t_1^2[3 + 2\delta_1(\boldsymbol{k})] \\ & + 4t_2^2(\sin^2\phi)\ [\delta_2(\boldsymbol{k})]^2 - 4Mt_2(\sin\phi)\delta_2(\boldsymbol{k}), \end{aligned} \tag{S29}$$

and

$$\begin{aligned} \delta_1(\boldsymbol{k}) &:= \textstyle\sum_i \cos\boldsymbol{k}\cdot\boldsymbol{b}_i = 2\cos\frac{3k_1}{2}\cos\frac{\sqrt{3}k_2}{2} + \cos\sqrt{3}k_2, \\ \delta_2(\boldsymbol{k}) &:= \textstyle\sum_i \sin\boldsymbol{k}\cdot\boldsymbol{b}_i = -2\cos\frac{3k_1}{2}\sin\frac{\sqrt{3}k_2}{2} + \sin\sqrt{3}k_2. \end{aligned} \tag{S30}$$

The operators $c_{\boldsymbol{k}}$ and $d_{\boldsymbol{k}}$ are related to $a_{\boldsymbol{k}}$ and $b_{\boldsymbol{k}}$ via the canonical transformation

$$\begin{pmatrix} a_{\boldsymbol{k}} \\ b_{\boldsymbol{k}} \end{pmatrix} = \frac{1}{\sqrt{1+|x_{\boldsymbol{k}}|^2}} \begin{pmatrix} x_{\boldsymbol{k}} & 1 \\ -1 & x_{\boldsymbol{k}}^* \end{pmatrix} \begin{pmatrix} c_{\boldsymbol{k}} \\ d_{\boldsymbol{k}} \end{pmatrix}, \tag{S31}$$

where

$$x_{\boldsymbol{k}} := \frac{t_1 \sum_i \mathrm{e}^{-\mathrm{i}\boldsymbol{k}\cdot\boldsymbol{a}_i}}{M - 2t_2(\sin\phi)\ \delta_2(\boldsymbol{k}) + \sqrt{\Delta(\boldsymbol{k})}}. \tag{S32}$$

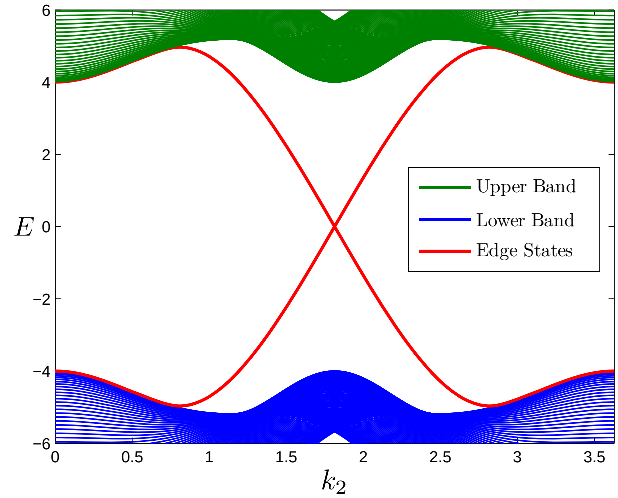

Figure S2: Energy bands of the Hamiltonian (S35) as a function of the momentum k_2. The red lines correspond to the edge state modes. The rest of parameters are $M = 0$, $\phi = \pi/2$ and $t_1 = 4$ (in units of $t_2 = 1$).

b. *Cylindrical Geometry*

In this case we take periodic boundary conditions along the direction $\boldsymbol{a}_2$ and open boundaries along $\boldsymbol{a}_1$, so that we work with a cylindrical configuration. The inverse Fourier transform along the $\boldsymbol{a}_2$ direction of the fermionic operators is given by

$$a_{(m,n)} = \frac{1}{\sqrt{N_2}} \sum_{k_2\in\text{B.Z.}} \mathrm{e}^{\mathrm{i}k_2 n|\boldsymbol{a}_2|} a_{(m,k_2)}, \tag{S33}$$

$$b_{(m,n)} = \frac{1}{\sqrt{N_2}} \sum_{k_2\in\text{B.Z.}} \mathrm{e}^{\mathrm{i}k_2 n|\boldsymbol{a}_2|} b_{(m,k_2)}, \tag{S34}$$

where the Brillouin zone corresponds to the interval $k_2 \in (-\pi/|\boldsymbol{a}_2|, \pi/|\boldsymbol{a}_2|) = (-\pi/\sqrt{3}, \pi/\sqrt{3})$, and N_2 is the number of two-site basic cells along the direction $\boldsymbol{a}_2$. By using these equations in the Hamiltonian (S19) we obtain

$$\begin{aligned} H_{\rm s} = \sum_{k_2\in\text{B.Z}} \sum_m \Bigg(& \left[\tfrac{M}{2} + t_2\cos\left(\sqrt{3}k_2 - \phi\right)\right] a_{(m,k_2)}^\dagger a_{(m,k_2)} \\ & + \left[-\tfrac{M}{2} + t_2\cos(\sqrt{3}k_2 + \phi)\right] b_{(m,k_2)}^\dagger b_{(m,k_2)} \\ & + t_1\left[a_{(m+1,k_2)}^\dagger b_{(m,k_2)} + \left(1 + \mathrm{e}^{\mathrm{i}\sqrt{3}k_2}\right) a_{(m,k_2)}^\dagger b_{(m,k_2)}\right] \\ & + t_2\Big[\left(\mathrm{e}^{\mathrm{i}(\sqrt{3}k_2+\phi)} + \mathrm{e}^{-\mathrm{i}\phi}\right) a_{(m,k_2)}^\dagger a_{(m+1,k_2)} \\ & + \left(\mathrm{e}^{\mathrm{i}(\sqrt{3}k_2-\phi)} + \mathrm{e}^{\mathrm{i}\phi}\right) b_{(m,k_2)}^\dagger b_{(m+1,k_2)}\Big] + \text{h.c.}\Bigg). \end{aligned} \tag{S35}$$

This Hamiltonian has the structure $H_{\rm s} = \sum_{k_2\in\text{B.Z.}} H(k_2)$, therefore we can diagonalize H by diagonalizing each $H(k_2)$. In Fig. S2 we have depicted

the behaviour of the eigenvalues of $H(k_2)$ as a function of k_2. The red lines connecting the upper and lower bands correspond to the edge state modes, which are localized on the edges of the direction $\boldsymbol{a}_1$.

4. Derivation of the Master Equation for the Haldane Model

In this section we derive the dynamical equation (master equation) for the Haldane model coupled to a thermal bath. We assume the usual condition of weak system-bath coupling, which is a standard assumption for thermalization.

The total Hamiltonian of the problem considered reads as follows

$$H := H_{\mathrm{s}} + H_{\mathrm{b}} + H_{\mathrm{s-b}}. \tag{S36}$$

The first term, H_{s}, is the Haldane Hamiltonian (S19). The second term in (S36), H_{b}, is the free Hamiltonian of the local baths,

$$H_{\mathrm{b}} := \sum_{i,\boldsymbol{r}} \epsilon^i \left(A_{\boldsymbol{r}}^{i\dagger} A_{\boldsymbol{r}}^i + B_{\boldsymbol{r}}^{i\dagger} B_{\boldsymbol{r}}^i \right), \tag{S37}$$

where A and B stand for independent fermionic bath operators that satisfy the canonical anti-commutation relations $\{A_n^i, A_{n'}^{j\dagger}\} = \delta_{n,n'}\delta_{i,j}$, $\{A_n^i, A_{n'}^j\} = 0$ and analogously for B_n^i. The index $\boldsymbol{r}$ denotes the position of the local bath on the lattice and i runs over the bath degrees of freedom. Also, ϵ^i represents the energy of each mode i of the bath which is assumed to be independent of the lattice site. Finally, the third term in (S36), $H_{\mathrm{s-b}}$, is given by

$$H_{\mathrm{s-b}} := \sum_{i,\boldsymbol{r}} g^i (a_{\boldsymbol{r}}^\dagger \otimes A_{\boldsymbol{r}}^i + a_{\boldsymbol{r}} \otimes A_{\boldsymbol{r}}^{i\dagger} + b_{\boldsymbol{r}}^\dagger \otimes B_{\boldsymbol{r}}^i + b_{\boldsymbol{r}} \otimes B_{\boldsymbol{r}}^{i\dagger}), \tag{S38}$$

and describes an exchange of fermions between system and bath mediated by a coupling constant g^i which may depend on the specific mode i of the baths.

The total dynamics of system and bath is given by the Liouville-Von-Neumann equation:

$$\frac{d\rho}{dt} = -\mathrm{i}[H, \rho]. \tag{S39}$$

After taking the interaction picture with respect to $H_0 = H_{\mathrm{s}} + H_{\mathrm{b}}$,

$$\frac{d\tilde{\rho}}{dt} = -\mathrm{i}[\tilde{H}_{\mathrm{s-b}}, \tilde{\rho}] \quad \text{with} \begin{cases} \tilde{\rho} := \mathrm{e}^{\mathrm{i}H_0 t} \rho \mathrm{e}^{-\mathrm{i}H_0 t}, \\ \tilde{H}_{\mathrm{s-b}} := \mathrm{e}^{\mathrm{i}H_0 t} H_{\mathrm{s-b}} \mathrm{e}^{-\mathrm{i}H_0 t}. \end{cases} \tag{S40}$$

For small $\tilde{H}_{\mathrm{s-b}}$ the system dynamics is approximately given (see [5–8]) by the equation

$$\frac{d\tilde{\rho}_{\mathrm{s}}}{dt} = -\int_0^\infty ds\ \mathrm{Tr}_{\mathrm{b}}[\tilde{H}_{\mathrm{s-b}}(t), [\tilde{H}_{\mathrm{s-b}}(t-s), \tilde{\rho}_{\mathrm{s}}(t) \otimes \rho_{\mathrm{b}}^\beta]], \tag{S41}$$

where Tr_{b} denotes the trace over the bath degrees of freedom and ρ_{b}^β is the initial state of the bath, which we assumed to be the Gibbs state

$$\rho_{\mathrm{b}}^\beta := \frac{\mathrm{e}^{-\beta H_{\mathrm{b}}}}{Z}. \tag{S42}$$

a. *Toroidal geometry*

We consider periodic boundary conditions and take Fourier transforms in the Hamiltonian (S36). For the first term we obtain (S24), for the second we have

$$H_{\mathrm{b}} = \sum_{i,\boldsymbol{k}} \epsilon^i \left(A_{\boldsymbol{k}}^{i\dagger} A_{\boldsymbol{k}}^i + B_{\boldsymbol{k}}^{i\dagger} B_{\boldsymbol{k}}^i \right), \tag{S43}$$

and finally for the interaction term

$$H_{\mathrm{s-b}} = \sum_{i,\boldsymbol{k}} g^i (a_{\boldsymbol{k}}^\dagger \otimes A_{\boldsymbol{k}}^i + a_{\boldsymbol{k}} \otimes A_{\boldsymbol{k}}^{i\dagger} + b_{\boldsymbol{k}}^\dagger \otimes B_{\boldsymbol{k}}^i + b_{\boldsymbol{k}} \otimes B_{\boldsymbol{k}}^{i\dagger}). \tag{S44}$$

Let us stress again that the strength of the coupling to each mode of the bath is represented by g^i. This, analogously to the energy of each mode ϵ^i, is taken to be independent of the lattice site and of the type of bath A or B, which is rather natural.

In terms of the operators $c_{\boldsymbol{k}}$ and $d_{\boldsymbol{k}}$ the Hamiltonian (S44) reads

$$H_{\mathrm{s-b}} = \sum_{i,\boldsymbol{k}} g^i (c_{\boldsymbol{k}}^\dagger \otimes C_{\boldsymbol{k}}^i + c_{\boldsymbol{k}} \otimes C_{\boldsymbol{k}}^{i\dagger} + d_{\boldsymbol{k}}^\dagger \otimes D_{\boldsymbol{k}}^i + d_{\boldsymbol{k}} \otimes D_{\boldsymbol{k}}^{i\dagger}). \tag{S45}$$

where

$$\begin{pmatrix} C_{\boldsymbol{k}}^i \\ D_{\boldsymbol{k}}^i \end{pmatrix} = \frac{1}{\sqrt{1+|x_{\boldsymbol{k}}|^2}} \begin{pmatrix} x_{\boldsymbol{k}}^* & -1 \\ 1 & x_{\boldsymbol{k}} \end{pmatrix} \begin{pmatrix} A_{\boldsymbol{k}}^i \\ B_{\boldsymbol{k}}^i \end{pmatrix} \tag{S46}$$

are new fermionic modes of the bath. Moreover note that

$$H_{\mathrm{b}} = \sum_{i,\boldsymbol{k}} \epsilon^i \left(C_{\boldsymbol{k}}^{i\dagger} C_{\boldsymbol{k}}^i + D_{\boldsymbol{k}}^{i\dagger} D_{\boldsymbol{k}}^i \right). \tag{S47}$$

Now, it is easy to write $H_{\mathrm{s-b}}$ in the interaction picture and apply the formula (S41), which can be quite simplified by using that

$$\begin{aligned} \mathrm{Tr}_{\mathrm{b}}(C_{\boldsymbol{k'}}^{j\dagger} C_{\boldsymbol{k}}^i \rho_\beta) &= \mathrm{Tr}_{\mathrm{b}}(D_{\boldsymbol{k'}}^{j\dagger} D_{\boldsymbol{k}}^i \rho_\beta) = \bar{n}_F(\epsilon^i)\delta_{i,j}\delta_{\boldsymbol{k},\boldsymbol{k'}}, \\ \mathrm{Tr}_{\mathrm{b}}(C_{\boldsymbol{k'}}^{j} C_{\boldsymbol{k}}^{i\dagger} \rho_\beta) &= \mathrm{Tr}_{\mathrm{b}}(D_{\boldsymbol{k'}}^{j} D_{\boldsymbol{k}}^{i\dagger} \rho_\beta) = [1-\bar{n}_F(\epsilon^i)]\delta_{i,j}\delta_{\boldsymbol{k},\boldsymbol{k'}}, \\ \mathrm{Tr}_{\mathrm{b}}(C_{\boldsymbol{k'}}^{j\dagger} D_{\boldsymbol{k}}^i \rho_\beta) &= \mathrm{Tr}_{\mathrm{b}}(D_{\boldsymbol{k'}}^{j\dagger} C_{\boldsymbol{k}}^i \rho_\beta) = 0. \end{aligned}$$

Here, $\bar{n}_F(E) := \frac{1}{\mathrm{e}^{\beta E}+1}$ is the mean number of particles of the Fermi-Dirac distribution, where we have taken the chemical potential μ to be at the origin of the energy. In the continuous limit for the baths degrees of freedom we have

$$\sum_i (g^i)^2 f(\epsilon^i) \longrightarrow \int d\epsilon J(\epsilon) f(\epsilon), \tag{S48}$$

for any function $f(\epsilon)$, where $J(\omega)$ is the so-called spectral density of the bath. Thus, the Sokhotsky's identity

$$\int_0^\infty d\tau \mathrm{e}^{\mathrm{i}\omega\tau} = \pi\delta(\omega) + \mathrm{i}\mathrm{PV}\left(\frac{1}{\omega}\right) \tag{S49}$$

allows us to simplify further the final expression, which after a bit long but straightforward computation reads

$$\begin{aligned}\frac{d\rho_{\rm s}(t)}{dt} &= \sum_{\boldsymbol{k}} \mathcal{L}_{\boldsymbol{k}}[\rho_{\rm s}(t)] = \sum_{\boldsymbol{k}} \Bigg(-\mathrm{i}[H_{\boldsymbol{k}}, \rho_{\rm s}(t)] \\ &+ \gamma(E_1^{\boldsymbol{k}})\bar{n}_F(E_1^{\boldsymbol{k}})\Big(c^\dagger_{\boldsymbol{k}}\rho_{\rm s}(t)c_{\boldsymbol{k}} - \frac{1}{2}\{c_{\boldsymbol{k}}c^\dagger_{\boldsymbol{k}},\ \rho_{\rm s}(t)\}\Big) + \\ &+ \gamma(E_1^{\boldsymbol{k}})[1-\bar{n}_F(E_1^{\boldsymbol{k}})]\Big(c_{\boldsymbol{k}}\rho_{\rm s}(t)c^\dagger_{\boldsymbol{k}} - \frac{1}{2}\{c^\dagger_{\boldsymbol{k}}c_{\boldsymbol{k}}, \rho_{\rm s}(t)\}\Big) \\ &+ \gamma(E_2^{\boldsymbol{k}})\bar{n}_F(E_2^{\boldsymbol{k}})\Big(d^\dagger_{\boldsymbol{k}}\rho_{\rm s}(t)d_{\boldsymbol{k}} - \frac{1}{2}\{d_{\boldsymbol{k}}d^\dagger_{\boldsymbol{k}}, \rho_{\rm s}(t)\}\Big) + \\ &+ \gamma(E_2^{\boldsymbol{k}})[1-\bar{n}_F(E_2^{\boldsymbol{k}})]\Big(d_{\boldsymbol{k}}\rho_{\rm s}(t)d^\dagger_{\boldsymbol{k}} - \frac{1}{2}\{d^\dagger_{\boldsymbol{k}}d_{\boldsymbol{k}},\ \rho_{\rm s}(t)\}\Big)\Bigg),\end{aligned} \tag{S50}$$

in Schödinger picture, where $\gamma(\omega) := 2\pi J(\omega)$. In addition, in this equation we have neglected the imaginary parts of Eq. (S49) because they represent just a small shift of energies which does not affect to the dissipative process [9].

b. Cylindrical geometry

In this case, we take Fourier transform along the direction $\boldsymbol{a}_2$ in (S36). Thus, the Haldane Hamiltonian reads as (S35), the bath Hamiltonian becomes

$$H_{\rm b} = \sum_{k_2}\sum_{i,m} \epsilon^i \left(A^{i\dagger}_{(m,k_2)}A^i_{(m,k_2)} + B^{i\dagger}_{(m,k_2)}B^i_{(m,k_2)}\right), \tag{S51}$$

and the interaction Hamiltonian

$$\begin{aligned}H_{\rm s-b} = \sum_{k_2\in \rm B.Z.}\sum_{i,m} g^i \Big(& a^\dagger_{(m,k_2)}\otimes A^i_{(m,k_2)} + a_{(m,k_2)}\otimes A^{i\dagger}_{(m,k_2)} \\ &+ b^\dagger_{(m,k_2)}\otimes B^i_{(m,k_2)} + b_{(m,k_2)}\otimes B^{i\dagger}_{(m,k_2)}\Big).\end{aligned} \tag{S52}$$

where m runs from 1 to the number of two-sites basic cells along the direction $\boldsymbol{a}_1$, N_1.

We may collect the operators a_m and b_m of each site in a new operator c_m where $c_1 := a_1$, $c_2 := b_1$, $c_3 := a_2$, $c_4 := b_2$ and so on. The same can be done for the baths operators A and B with the notation C_m. Then, the interaction Hamiltonian (S52) is written as

$$H_{\rm s-b} = \sum_{k_2\in \rm B.Z.}\sum_{i,m} g^i \Big(c^\dagger_{(m,k_2)}\otimes C^i_{(m,k_2)} + c_{(m,k_2)}\otimes C^{i\dagger}_{(m,k_2)}\Big). \tag{S53}$$

where now m runs from 1 to $2N_1$.

The diagonal modes $f_{(m,k_2)}$ of $H(k_2) = \sum_m E_m(k_2) f^\dagger_{(m,k_2)}f_{(m,k_2)}$, where $E_m(k_2)$ is depicted in Fig. S2, are related to $c_{(m,k_2)}$ by some unitary transformation

$$c_{(m,k_2)} = \sum_\ell w^{k_2}_{m,\ell} f_{(\ell,k_2)}, \quad \text{with } \sum_\ell w^{k_2 *}_{\ell,m} w^{k_2}_{\ell,m'} = \delta_{m,m'}. \tag{S54}$$

By using this equation in (S53) and after a bit of algebra we arrive at

$$H_{\rm s-b} = \sum_{i,m,k_2} g^i \Big(f^\dagger_{(m,k_2)}\otimes F^i_{(m,k_2)} + f_{(m,k_2)}\otimes F^{i\dagger}_{(m,k_2)}\Big), \tag{S55}$$

where

$$F^i_{(m,k_2)} := \sum_\ell w^{k_2 *}_{\ell,m} C^i_{(\ell,k_2)}, \tag{S56}$$

are new fermionic bath modes.

Following the same steps as for the toroidal geometry, it is not difficult to obtain the master equation of the cylindrical array,

$$\begin{aligned}\frac{d\rho_{\rm s}(t)}{dt} &= \sum_{k_2\in \rm B.Z.} \mathcal{L}_{k_2}[\rho_{\rm s}(t)] = \sum_{k_2\in \rm B.Z.} \Bigg(-\mathrm{i}[H(k_2), \rho_{\rm s}(t)] \\ &+ \sum_m \Big(\gamma\big(E^{k_2}_m\big)\bar{n}_F\big(E^{k_2}_m\big)\mathcal{D}_{f^\dagger_{(m,k_2)}}[\rho_{\rm s}(t)] \\ &+ \gamma\big(E^{k_2}_m\big)\big[1-\bar{n}_F\big(E^{k_2}_m\big)\big]\mathcal{D}_{f_{(m,k_2)}}[\rho_{\rm s}(t)]\Big)\Bigg),\end{aligned} \tag{S57}$$

where

$$\mathcal{D}_K[\rho_{\rm s}(t)] := K\rho_{\rm s}(t)K^\dagger - \frac{1}{2}\{K^\dagger K, \rho_{\rm s}(t)\}. \tag{S58}$$

5. Steady State for the Haldane Model

a. Toroidal Geometry

The steady state of the previous band Liouvillian (S50) is the Gibbs state of the Hamiltonian $H_{\rm s}$,

$$\rho_\beta = \frac{\mathrm{e}^{-\beta H_{\rm s}}}{Z}, \tag{S59}$$

where $\beta = 1/T$, with T the temperature of the fermionic bath, and $Z = \mathrm{Tr}(\mathrm{e}^{-\beta H_{\rm s}})$ the partition function. To prove this, first note that $[H_{\rm s}, \rho_\beta] = 0$ so we just need to care about the dissipator in (S50). In addition, since the number operators $c^\dagger_{\boldsymbol{k}}c_{\boldsymbol{k}}$ and $d^\dagger_{\boldsymbol{k}}d_{\boldsymbol{k}}$ commute with $c^\dagger_{\boldsymbol{k}'}$, $c_{\boldsymbol{k}'}$, $d^\dagger_{\boldsymbol{k}'}$, and $d_{\boldsymbol{k}'}$ if $\boldsymbol{k}\neq\boldsymbol{k}'$, and we are left only with the part where the crystalline momenta in $\mathcal{L}_{\boldsymbol{k}}$ and $\rho^{\boldsymbol{k}}_{\rm ss}$ are the same, as the others trivially vanish. Since

$$\mathrm{e}^{\beta E}\bar{n}_F(E) = [1-\bar{n}_F(E)], \tag{S60}$$

and

$$\rho_{\rm ss}^{\boldsymbol{k}} = \left(\frac{\mathrm{e}^{-\beta E_1^{\boldsymbol{k}} c_{\boldsymbol{k}}^\dagger c_{\boldsymbol{k}}}}{1+\mathrm{e}^{-\beta E_1^{\boldsymbol{k}}}}\right)\left(\frac{\mathrm{e}^{-\beta E_2^{\boldsymbol{k}} d_{\boldsymbol{k}}^\dagger d_{\boldsymbol{k}}}}{1+\mathrm{e}^{-\beta E_2^{\boldsymbol{k}}}}\right), \tag{S61}$$

it is easy to proof that

$$\begin{aligned}\mathcal{L}_{\boldsymbol{k}}(\rho_{\rm ss}^{\boldsymbol{k}}) &= \bar{n}_F(E)\left(c_{\boldsymbol{k}}\rho_{\rm ss}^{\boldsymbol{k}}c_{\boldsymbol{k}}^\dagger - \frac{1}{2}\{c_{\boldsymbol{k}}^\dagger c_{\boldsymbol{k}}, \rho_{\rm ss}^{\boldsymbol{k}}\}\right)\\ &- [1-\bar{n}_F(E)]\left(c_{\boldsymbol{k}}\rho_{\rm ss}^{\boldsymbol{k}}c_{\boldsymbol{k}}^\dagger - \frac{1}{2}\{c_{\boldsymbol{k}}^\dagger c_{\boldsymbol{k}}, \rho_{\rm ss}^{\boldsymbol{k}}\}\right)\\ &+ \bar{n}_F(E)\left(d_{\boldsymbol{k}}\rho_{\rm ss}^{\boldsymbol{k}}d_{\boldsymbol{k}}^\dagger - \frac{1}{2}\{d_{\boldsymbol{k}}^\dagger d_{\boldsymbol{k}}, \rho_{\rm ss}^{\boldsymbol{k}}\}\right)\\ &- [1-\bar{n}_F(E)]\left(d_{\boldsymbol{k}}\rho_{\rm ss}^{\boldsymbol{k}}d_{\boldsymbol{k}}^\dagger - \frac{1}{2}\{d_{\boldsymbol{k}}^\dagger d_{\boldsymbol{k}}, \rho_{\rm ss}^{\boldsymbol{k}}\}\right) = 0.\end{aligned} \tag{S62}$$

Moreover, the state ρ_β is the unique steady state of (S50) as the interaction Hamiltonian (S38) satisfies the irreducibility condition presented in [10].

In order to analyze some properties of ρ_β, let us write the density matrix $\rho_{\rm ss}^{\boldsymbol{k}}$ in the occupation basis of the two bands for a fixed momentum $\boldsymbol{k}$. The basis reads as $|ij\rangle_{\boldsymbol{k}}$, where $i = 0, 1$ and $j = 0, 1$ stand for the occupation of one-particle state in the lower and upper band respectively. Thus, $\rho_{\rm ss}^{\boldsymbol{k}}$ is a 4×4 diagonal matrix,

$$\rho_{\rm ss}^{\boldsymbol{k}} = \mathrm{diag}\left(p_{0000}^{\boldsymbol{k}}, p_{1010}^{\boldsymbol{k}}, p_{0101}^{\boldsymbol{k}}, p_{1111}^{\boldsymbol{k}}\right) \tag{S63}$$

with

$$\begin{aligned} p_{0000}^{\boldsymbol{k}} &:= \left[(1+\mathrm{e}^{-\beta E_1^{\boldsymbol{k}}})(1+\mathrm{e}^{-\beta E_2^{\boldsymbol{k}}})\right]^{-1},\\ p_{1010}^{\boldsymbol{k}} &:= p_{0000}^{\boldsymbol{k}}\mathrm{e}^{-\beta E_1^{\boldsymbol{k}}},\\ p_{0101}^{\boldsymbol{k}} &:= p_{0000}^{\boldsymbol{k}}\mathrm{e}^{-\beta E_2^{\boldsymbol{k}}},\\ p_{1111}^{\boldsymbol{k}} &:= p_{0000}^{\boldsymbol{k}}\mathrm{e}^{-\beta E_1^{\boldsymbol{k}}}\mathrm{e}^{-\beta E_2^{\boldsymbol{k}}}. \end{aligned} \tag{S64}$$

Since we set the origin of energy at $E_0 = 0$ and also took the chemical potential $\mu = 0$ in between the two bands, $E_1^{\boldsymbol{k}} < 0, E_2^{\boldsymbol{k}} > 0$. Thus, at the low temperature limit, the state $\rho_{\rm ss}^{\boldsymbol{k}} \to |10\rangle_{\boldsymbol{k}}$ as $T \to 0$ K. This means that at $T = 0$ K the lower band is fully occupied and the upper band is completely empty, that is actually what one may expect. At the opposite limit, for $T\to\infty$, the system gets completely mixed, as the four possible states can be equally populated by the environment.

For the sake of clarity, we write the members of the occupation basis as

$$\begin{aligned} |00\rangle_{\boldsymbol{k}} &= |0\rangle|0\rangle,\\ |10\rangle_{\boldsymbol{k}} &= |u_{c,\boldsymbol{k}}\rangle|0\rangle,\\ |01\rangle_{\boldsymbol{k}} &= |0\rangle|u_{d,\boldsymbol{k}}\rangle,\\ |11\rangle_{\boldsymbol{k}} &= |u_{c,\boldsymbol{k}}\rangle|u_{d,\boldsymbol{k}}\rangle. \end{aligned}$$

Then by using Eqs. (9) and (S12), we obtain (note that the $\partial_i|0\rangle = 0$ as by definition the vacuum has no particles and so it does not depend on $\boldsymbol{k}$)

$$A_i^\rho(\boldsymbol{k}) = p_{1010}^{\boldsymbol{k}}A_i^c(\boldsymbol{k}) + p_{0101}^{\boldsymbol{k}}A_i^d(\boldsymbol{k}) + p_{1111}^{\boldsymbol{k}}(A_i^c(\boldsymbol{k}) + A_i^d(\boldsymbol{k})). \tag{S65}$$

where the Berry connections for the lower c and upper d bands are provided by

$$A_i^\alpha(\boldsymbol{k}) = \mathrm{i}\langle u_{\alpha,\boldsymbol{k}}|\partial_i u_{\alpha,\boldsymbol{k}}\rangle, \quad \alpha = c, d. \tag{S66}$$

Thus, the expressions for $p_{ijkl}^{\boldsymbol{k}}$ given in Eq. (S64) lead to

$$A_i^\rho(\boldsymbol{k}) = \bar{n}_F(E_1^{\boldsymbol{k}})A_i^c(\boldsymbol{k}) + \bar{n}_F(E_2^{\boldsymbol{k}})A_i^d(\boldsymbol{k}). \tag{S67}$$

b. *Cylindrical Geometry*

Because of the same reasons as with the toroidal geometry, the master equation on a cylindrical geometry (S57) has a unique steady state, which is the Gibbs state at the same temperature as the bath

$$\rho_\beta = \frac{\mathrm{e}^{-\beta\sum_{k_2}H(k_2)}}{Z} = \bigotimes_{k_2}\frac{\mathrm{e}^{-\beta H(k_2)}}{Z_{k_2}}, \tag{S68}$$

with $Z_{k_2} = \mathrm{Tr}\left[\mathrm{e}^{-\beta H(k_2)}\right]$. Provided the system exhibits topological order, this state can be split as

$$\rho_\beta(k_2) = \frac{\mathrm{e}^{-\beta H(k_2)}}{Z_{k_2}} = \rho_\beta^{\rm L}(k_2)\otimes\rho_\beta^{\rm bulk}(k_2)\otimes\rho_\beta^{\rm R}(k_2), \tag{S69}$$

where

$$\rho_\beta^{\rm L,R}(k_2) := \frac{\mathrm{e}^{-\beta E_{L,R}(k_2)f^\dagger_{(L,R,k_2)}f_{(L,R,k_2)}}}{1+\mathrm{e}^{-\beta E_{L,R}(k_2)}}, \tag{S70}$$

are Gibbs states involving just the gapless edge modes depicted in Fig. S2.

[1] M. A. Nielsen and I. L. Chuang, *Quantum Computation and Quantum Information* (Cambridge University Press, Cambridge, 2000).
[2] M. V. Berry, Proc. R. Soc. A **392**, 45 (1984).
[3] T. Eguchi, P. B. Gilkey and A. J. Hanson, Phys. Rep. **66**, 213 (1980).
[4] F.D.M. Haldane, Phys. Rev. Lett. **61**, 2015 (1988).
[5] R. Alicki and K. Lendi, *Quantum Dynamical Semigroups and Applications* (Springer, Berlin, 1987).
[6] C.W. Gardiner and P. Zoller, *Quantum Noise* (Springer, Berlin, 1991 Third Edition).
[7] H.-P. Breuer and F. Petruccione, *The Theory of Open*

Quantum Systems (Oxford University Press, 2002).
[8] A. Rivas and S.F. Huelga, *Open Quantum Systems. An Introduction* (Springer, Heidelberg, 2011).
[9] A. Rivas, A. D. K. Plato, S. F. Huelga and M. B. Plenio, New J. Phys. **12**, 113032 (2010).
[10] H. Spohn, Lett. Math. Phys. **2**, 33 (1977).